Asian Journal of Chemistry; Vol. 37, No. 2 (2025), 331-339

ASIAN JOURNAL OF CHEMISTRY

https://doi.org/10.14233/ajchem.2025.33029

Synthesis and Antioxidant Potential of Novel Benzimidazole Derivatives: A Comparative Study of Experimental and DFT Insights

RAJIV MALL[1,*], MANINDER KAUR[2] and VARINDER SINGH[3]

[1]Department of Chemistry, Punjabi University, Patiala-147002, India
[2]Department of Physics, Punjabi University, Patiala-147002, India
[3]Department of Chemistry, RIMT University, Mandi Gobindgarh, Fatehgarh Sahib-147301, India

*Corresponding author: E-mail: rajivmall@pbi.ac.in

Received: 12 November 2024; *Accepted*: 21 December 2024; *Published online*: 31 January 2025; AJC-21883

Benzimidazole based novel compounds were synthesized and characterized using NMR, FTIR and mass spectrometry. Quantum computations, encompassing optimized structure, FTIR and NMR analyses, were conducted through density functional theory (DFT) employing the B3LYP/6-311G(d,p) basis set. Compounds with the oxygen linker (**6a** and **6b**) exhibit higher ZPVE (zero-point vibrational energy) and dipole moments than those with a direct linker, while chlorobenzyl-substituted compounds (**6b** and **7b**) have higher dipole moments than their benzyl counterparts. The strong correlation ($R^2 \approx 1$) between experimental and computed ^{1}H NMR and FTIR spectra confirms the accuracy of the B3LYP method. Among them, compound **7b** shows the highest softness (0.927 eV^{-1}), the smallest HOMO-LUMO gap (2.158 eV) and the best antioxidant potency ($EC_{50} = 0.316 \pm 0.001$ mM), making it the most promising compound. This study underscores the pharmacological potential of the synthesized benzimidazole derivatives for future development.

Keywords: Benzimidazole derivatives, Antioxidant study, Zero-point vibrational energy, HOMO-LUMO gap, Dipole moment.

INTRODUCTION

Benzimidazole derivatives represent an important class of heterocyclic compounds due to their diverse biological activities and wide range of pharmacological applications. These compounds have gained significant attention in the field of medicinal chemistry, where they exhibit activities such as antimicrobial, antiviral, antidiabetic, antioxidants and anticancer activity [1,2]. The structural framework of benzimidazole provides a versatile scaffold for the synthesis of novel compounds, which are capable of interacting with various biological targets due to their heteroatom-rich nature and ability to participate in hydrogen bonding and π-π stacking interactions [3,4].

Among the numerous pharmacological properties of benzimidazole derivatives, their antioxidant activity is of particular interest. Oxidative stress, which results from an imbalance between the production of free radicals and the antioxidant defense system, is implicated in various chronic diseases such as cancer, cardiovascular disorders and neurodegenerative diseases [5]. Antioxidants play a crucial role in neutralizing reactive oxygen species (ROS) and preventing cellular damage [6]. Benzimidazole derivatives, due to their electron-rich aromatic systems, have shown potential in scavenging free radicals and inhibiting oxidative processes, making them promising candidates for antioxidant therapy [7,8]. Several studies have shown that structural changes of benzimidazole, especially those involving substituents at 2-position, might improve its antioxidant activity [9-11], highlighting the importance of structure-activity relationship (SAR) studies in this domain.

In addition to the experimental evaluations, computational techniques, such as density functional theory (DFT) provide valuable insights into the electronic properties and reactivity of benzimidazole-based compounds [12,13]. DFT, particularly the B3LYP functional combined with 6-311G(d,p) basis set [14], has been widely used to optimize molecular geometries and predict various electronic parameters, including chemical hardness, electronegativity, softness, chemical potential and the HOMO-LUMO energy gap [15]. These parameters are critical in understanding the reactivity, stability and antioxidant potential of the molecules. The comparison between theoretical

and experimental spectroscopic data, such as nuclear magnetic resonance (NMR) and Fourier-transform infrared (FTIR) spectroscopy, further validates the structural integrity of synthesized compounds. Furthermore, DFT investigations offer a theoretical framework for elucidating antioxidant action, as the energy gap between HOMO and LUMO is frequently associated with a compound's ability to donate electrons to free radicals, a key mechanism in the antioxidant behaviour [16].

Herein, the synthesis of novel benzimidazoles and characterization using various spectroscopic techniques were carried out. The structures using DFT with the B3LYP/6-311G(d,p) basis set were further optimized and calculated several electronic parameters such as electronegativity, hardness, softness, chemical potential and the HOMO-LUMO gap. The antioxidant activity of the synthesized compounds was evaluated using the DPPH radical scavenging assay and the results were compared with the electronic properties obtained from DFT studies. A correlation was obtained between the theoretical predictions and experimental antioxidant activity, emphasizing the utility of DFT in predicting the bioactivity of synthesized novel benzimidazole derivatives.

EXPERIMENTAL

All the reagents utilized in this study were sourced from Aldrich and SD Fine Chemicals. The melting points were recorded using an open conc. H_2SO_4 bath and are uncorrected. Column chromatography and thin layer chromatography were carried out using silica gel 100-200 mesh (Loba Chemie) and silica gel GF_{254} (Loba Chemie), respectively. Spots in TLC was visualized using a UV cabinet (Perfit, India). The infrared spectra and NMR spectra of the synthesized compounds, were recorded using a Perkin-Elmer Spectrum RX FTIR spectrophotometer and a Bruker AC400F 400 MHz spectrometer, respectively, at SAIF, Panjab University, Chandigarh, India. The LC-MS data were obtained using a Waters Micromass Q-Tof Micro spectrometer, also at SAIF, Panjab University. The GC-MS analysis and elemental composition of the compounds were carried out using a Shimadzu GCMS-QP2010 Plus and a Vario Micro V1 Elemental Analyzer, respectively, at Instrumental Laboratory, Department of Chemistry, Punjabi University, Patiala, India. Compounds **1**, **2**, **3a** and **3b** were synthesized following procedures reported earlier [17,18].

Synthesis of intermediates and final compounds

General procedure for synthesis of N-substituted benzimidazolyl oxo-linked benzaldehyde (4a and 4b): A mixture of **3a/3b** (0.1 mol), 3-hydroxybenzaldehyde (0.1 mol), K_2CO_3 (0.3 mol) and CuI (catalytic amount) in pyridine was heated to 140 ºC for 22 h. The reaction mixture was allowed to cool, taken up in ethyl acetate (60 mL) and then washed three times with 0.5 N NaOH. The organic layer was dried (Na_2SO_4), filtered and concentrated under reduced pressure to give an oil which was subjected to column chromatography using a mixture of ethyl acetate/hexane (1:9) to afford the title compound **4a/4b** as white solid (**Scheme-I**).

3-[(1-Benzyl-1*H*-benzimidazol-2-yl)oxy]benzaldehyde (4a): White solid; yield: 70%; m.p.: 102-103 ºC; FTIR (KBr, ν_{max}, cm^{-1}): 2851, 2736 (OC-H), 1698 (C=O), 1450 (C=N), 1245 (C-O-C); ^1H NMR (400 MHz, $CDCl_3$) δ ppm: 10.14 (s, 1H, CHO), 7.88 (m, 1H, Ar), 7.78 (m, 1H, Ar), 7.67 (m, 1H, Ar), 7.62 (m, 2H, Ar), 7.36 (m, 5H, Ar), 7.20 (m, 3H, Ar), 5.35 (s, 2H, benzylic); ESI-MS (*m/z*): 329 $[M+1]^+$; Anal. calcd. (found) % for $C_{21}H_{16}N_2O_2$: C, 76.81 (76.44); H, 4.91 (5.15); N, 8.53 (8.01).

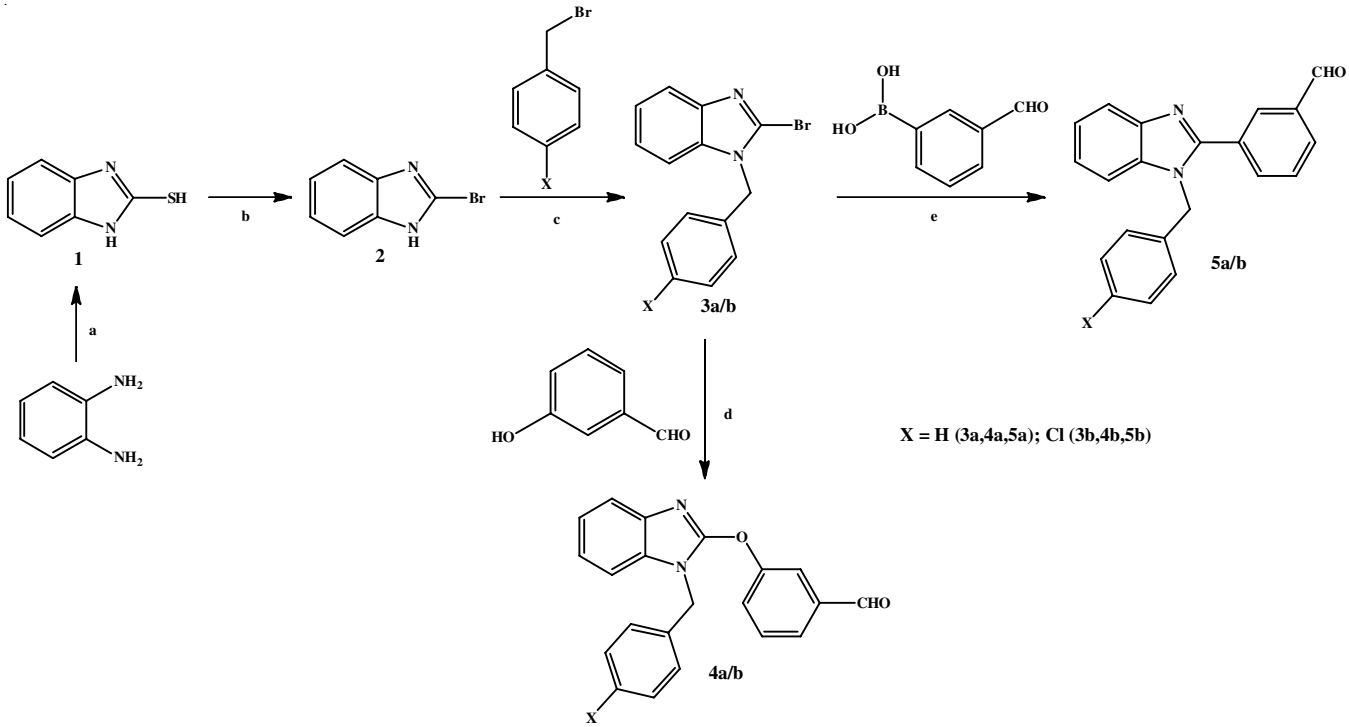

Scheme-I: Reagents and conditions: (a) carbon disulphide, ethanol, water, glacial acetic acid, Norit (b) HBr/glacial acetic acid, Br_2, water, NaOH (c) NaH/dry DMF (d) K_2CO_3, dry pyridine, CuI (e) $Pd(PPh_3)_4$, dioxane:water

3-{[1-(4-Chlorobenzyl)-1*H*-benzimidazol-2-yl]oxy}-benzaldehyde (4b): White solid; yield: 70%; m.p.: 110-111 ºC; FTIR (KBr, ν_{max}, cm^{-1}): 2838, 2732 (OC-H), 1699 (C=O), 1483 (C=N), 1247 (C-O-C), 801 (C-Cl); ^{1}H NMR (400 MHz, $CDCl_3$) δ ppm: 10.00 (s, 1H, CHO), 7.88 (d, *J* = 1.96 Hz, 1H, Ar), 7.87 (m, 1H, Ar), 7.67 (m, 1H, Ar), 7.58 (m, 2H, Ar), 7.29 (m, 2H, Ar), 7.18 (m, 5H, Ar), 5.30 (s, 2H, benzylic); ESI-MS (*m/z*): 362 $[M]^+$; Anal. calcd. (found) % for $C_{21}H_{15}N_2O_2Cl$: C, 69.52 (68.89); H, 4.17 (4.86); N, 7.72 (7.45).

General procedure for synthesis of *N*-substituted benzimidazolyl direct linked benzaldehyde (5a and 5b): To a solution of **3a/3b** (0.0225 mol) and 3-formylphenylboronic acid (0.015 mol) in a mixture of dioxane and water (4:1, 40 mL) was added K_2CO_3 (0.045 mol). The resulting mixture was degassed, stirred at ambient temperature for 20 min and catalytic amount (0.005 mmol) of $Pd(PPh_3)_4$ were added. The mixture was degassed again and then refluxed under nitrogen gas for 8 h. It was allowed to cool, filtered through celite and extracted using ethyl acetate (3 × 20 mL). The organic layer was dried (Na_2SO_4), filtered and concentrated under reduced pressure to give an oil which was subjected to column chromatography using a mixture of ethyl acetate/hexane (3:7) to afford the title compound **5a/5b** as white solid (**Scheme-I**).

4-(1-Benzyl-1*H*-benzimidazol-2-yl)benzaldehyde (5a): White solid; yield: 65%; m.p.: 150-152 ºC; FTIR (KBr, ν_{max}, cm^{-1}): 2811, 2721 (OC-H), 1704 (C=O), 1474 (C=N); ^{1}H NMR (400 MHz, $CDCl_3$) δ ppm: 9.90 (s, 1H, CHO), 8.12 (d, *J* = 1.20 Hz, 1H, Ar), 7.92 (d, *J* = 1.32 Hz, 1H, Ar), 7.90 (d, *J* = 1.32 Hz, 1H, Ar), 7.86 (m, 1H, Ar), 7.84 (m, 1H, Ar), 7.28 (m, 6H, Ar), 7.18 (m, 2H, Ar), 5.39 (s, 2H, benzylic); ESI-MS (*m/z*): 313 $[M+1]^+$; Anal. calcd. (found) % for $C_{21}H_{16}N_2O$: C, 80.75 (81.13); H, 5.16 (5.15); N, 8.97 (9.11).

3-[1-(4-Chlorobenzyl)-1*H*-benzimidazol-2-yl]benzaldehyde (5b): White solid; yield: 65%; m.p.: 162-165 ºC; FTIR (KBr, ν_{max}, cm^{-1}): 2850, 2729 (OC-H), 1730 (C=O), 1492 (C=N), 809 (C-Cl); ^{1}H NMR (400 MHz, $CDCl_3$) δ ppm: 10.02 (s, 1H, CHO), 8.20 (d, *J* = 1.52 Hz, 1H, Ar), 8.02 (d, *J* = 1.20 Hz, 1H, Ar), 8.01 (m, 2H, Ar), 8.00 (m, 1H, Ar), 7.92 (m, 1H, Ar), 7.88 (m, 3H, Ar), 7.38 (m, 1H, Ar), 7.04 (d, *J* = 8.48 Hz, 2H, Ar), 5.45 (s, 2H, benzylic); ESI-MS (*m/z*): 347 $[M]^+$; Anal. calcd. (found) % for $C_{21}H_{15}N_2OCl$: C, 72.73 (72.89); H, 4.36 (4.46); N, 8.08 (7.85).

General procedure for the synthesis of (6a, 6b, 7a and 7b): A mixture of compounds **4a/4b** or **5a/5b** (0.00075 mol), methylacetoacetate (0.00075 mol) and piperidinium acetate (0.15 mL) in toluene (20 mL) was refluxed for 10 h with continuous removal of water using a Dean-Stark trap. The crude reaction mixture was cooled to room temperature and concentrated to a viscous residue, which was purified by column chromatography using ethyl acetate/hexane as eluent to afford the title compound **6a/b** or **7a/b** (**Schemes II** and **III**).

Methyl 2-{3-[(1-benzyl-1*H*-benzimidazol-2-yl)oxy]benzylidene}-3-oxobutanoate (6a): Viscous mass; yield: 68%; FTIR (KBr, ν_{max}, cm^{-1}): 3441, 3007 (-$COOCH_3$), 3004 (-$COCH_3$), 2938 (-$COOCH_3$), 2857 (-$COCH_3$), 1719 and 1630 (C=O), 1523 (C=N), 1249 (C-O-C); ^{1}H NMR (400 MHz, $CDCl_3$) δ ppm:

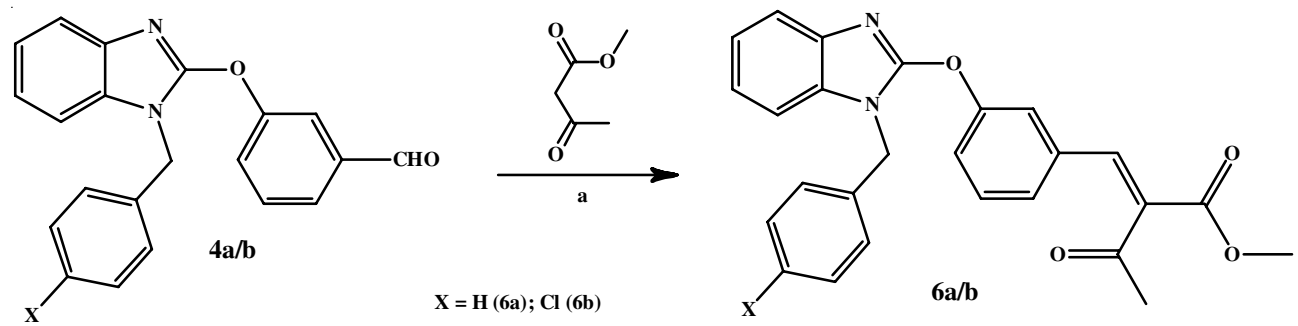

Scheme-II: Reagent and conditions: (a) piperidinium acetate, toluene

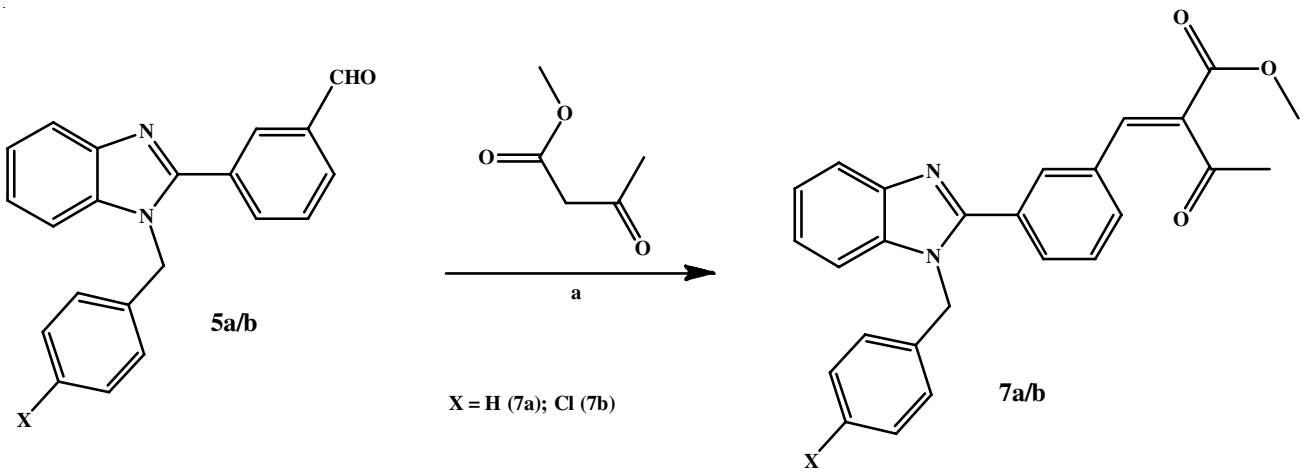

Scheme-III: Reagent and conditions: (a) piperidinium acetate, toluene

7.41 (m, 6H, Ar), 7.31 (m, 4H, Ar), 7.23 (s, 1H, benzylidenic), 7.21 (m, 3H, Ar), 5.32 (s, 2H, benzylic), 3.85 (s, 3H, -COOC$\underline{H}_3$), 2.41 (s, 3H, -COC$\underline{H}_3$); ESI-MS (*m/z*): 427 $[M+1]^+$, 467 $[M+23]^+$; Anal. calcd. (found) % for $C_{26}H_{22}N_2O_4$: C, 73.23 (72.91); H, 5.20 (5.43); N, 6.57 (6.25).

Methyl 2-{3-[(1-(4-chlorobenzyl)-1*H*-benzimidazol-2-yl)oxy]benzylidene}-3-oxobutanoate (6b): Viscous mass; yield: 62%; FTIR (KBr, ν_{max}, cm^{-1}): 2917 (-COOCH_3), 2849, 1724, 1699 (C=O), 1596 (C=N), 1238 (C-O-C), 804 (C-Cl); ^{1}H NMR (400 MHz, $CDCl_3$) δ ppm: 7.90 (d, *J* = 8.68 Hz, 2H, Ar), 7.88 (s, 1H, benzylidenic), 7.49 (d, *J* = 8.8 Hz, 2H, Ar), 7.39 (d, *J* = 8.8 Hz, 2H, Ar), 7.33 (m, 3H, Ar), 7.22 (m, 3H, Ar), 5.30 (s, 2H, benzylic), 3.85 (s, 3H, -COOC$\underline{H}_3$), 2.38 (s, 3H, -COC$\underline{H}_3$); ESI-MS (*m/z*): 461 $[M+1]^+$; Anal. calcd. (found) % for $C_{26}H_{21}N_2O_4Cl$: C, 67.75 (67.53); H, 5.59 (5.54); N, 6.06 (6.42).

Methyl 2-[3-(1-benzyl-1*H*-benzimidazol-2-yl)benzylidene]-3-oxobutanoate (7a): Viscous mass; yield: 75%; FTIR (KBr, ν_{max}, cm^{-1}): 3437, 2917 (-COOC$\underline{H}_3$), 2849, 1703 (C=O), 1485 (C=N), 1253 (C-O-C); ^{1}H NMR (400 MHz, $CDCl_3$) δ ppm: 7.85 (m, 1H, Ar), 7.58 (s, 1H, benzylidenic), 7.36 (m, 2H, Ar), 7.34 (m, 6H, Ar), 7.28 (m, 2H, Ar), 7.23 (m, 2H, Ar), 5.45 (s, 2H, benzylic), 2.27 (s, 3H, -COOC$\underline{H}_3$), 1.95 (s, 3H, -COC$\underline{H}_3$); ESI-MS (*m/z*): 410 $[M+1]^+$; Anal. calcd. (found) % for $C_{26}H_{22}N_2O_3$: C, 76.08 (76.27); H, 5.40 (5.25); N, 6.82 (7.07).

Methyl 2-{3-[1-(4-chlorobenzyl)-1*H*-benzimidazol-2-yl]benzylidene}-3-oxobutanoate (7b): Viscous mass; yield: 75%; FTIR (KBr, ν_{max}, cm^{-1}): 3020 (-COOCH_3), 2954 (-COCH_3), 2918 (-COOCH_3), 2850 (-COCH_3), 1705 (C=O), 1563 (C=N), 1252 (C-O-C), 807 (C-Cl); ^{1}H NMR (400 MHz, $CDCl_3$) δ ppm: 7.70 (d, *J* = 9.72 Hz, 1H, Ar-H), 7.48 (d, *J* = 8.28 Hz, 3H, Ar-H), 7.46 (m, 2H, Ar-H), 7.33 (m, 4H, Ar-H), 7.26 (s, 1H, benzylidenic), 7.03 (d, *J* = 8.44 Hz, 2H, Ar-H), 5.43 (s, 2H, benzylic), 3.86 (s, 3H, -COOC$\underline{H}_3$), 2.44 (s, 3H, -COC$\underline{H}_3$); ESI-MS (*m/z*): 445 $[M+1]^+$; Anal. calcd. (found) % for $C_{26}H_{21}N_2O_3Cl$: C, 70.19 (70.03); H, 4.76 (4.89); N, 6.30 (6.26).

DPPH assay: 2,2-Diphenyl-1-picrylhydrazyl (DPPH, 1 mg) was dissolved in 15 mL of methanol and its absorbance was recorded at 517 nm. To determine the percentage scavenging activity, varying concentrations of compounds **6a**-**7b** were prepared in MeOH, with five concentration levels for each compound: 0.033, 0.067, 0.100, 0.133 and 0.167 mM/L. For the antioxidant assay, 3 mL of freshly prepared DPPH solution was added to each concentration set, followed by 2 h incubation period. After incubation, the decrease in DPPH absorbance was measured using a UV-visible spectrophotometer at 517 nm. The radical scavenging activity was calculated using the following formula [11]:

$$\text{Scavenging activity } (\%) = \frac{A_o - A}{A_o} \times 100$$

where A_o = absorbance at 517 nm due to alone DPPH solution, A = absorbance at 517 nm after adding the antioxidants.

DFT study: Geometry optimizations and normal mode analysis were conducted using DFT calculations at the B3LYP/6-311G(d,p) level of theory with Gaussian 09. The absence of imaginary frequencies in the optimized geometry confirmed a true minimum on the potential energy surface. Molecular orbital energies and thermodynamic properties were also evaluated. The NMR chemical shifts were computed using the GIAO-IEFPCM method with the B3LYP/6-311G(d,p) basis set in DMSO. Theoretical NMR and FTIR results were then compared with experimental findings. Chemical potential (μ), electronegativity (χ), hardness (η), softness (S) and electrophilicity index (ω) can be calculated from the energies of HOMO and LUMO levels [15]:

$$\mu = \frac{E_{HOMO} + E_{LUMO}}{2}$$

$$\chi = -\frac{(E_{HOMO} + E_{LUMO})}{2}$$

$$\eta = \frac{E_{LUMO} - E_{HOMO}}{2}$$

$$S = \frac{1}{2\eta}$$

$$\omega = \frac{\mu^2}{2\eta}$$

RESULTS AND DISCUSSION

The *N*-benzyl/4-chlorobenzyl benzimidazol-2-yl based 3-substituted benzldehyde (**4a/4b**) with oxy linker was obtained by halide displacement from compound **3a/3b** by 3-hydroxybenzaldehyde (**Scheme-I**). Compound **3a/3b** in turn was obtained using commercially available 1,2-phenylenediamine through 2-mercaptobenzimidazole (**1**) and its subsequent bromination to compound **2** and *N*-benzylation/4-chlorobenzylation to compound **3a/3b**, respectively. The direct linked *N*-benzyl/4-chlorobenzyl benzimidazol-2-yl based 3-substituted benzaldehydes (**5a/5b**) was synthesized by Suzuki coupling of **3a/3b** with 3-formylphenylboronic acid (**Scheme-I**). All the targeted benzylidene based new chemical entities (NCEs) were synthesized in fairly good yields through Knoevenagel condensation of methyl acetoacetate with benzimidazole linked benzaldehydes (**4a/4b**) and (**5a/5b**) (**Scheme-II** and **III**) while using piperidinium acetate/toluene as base under reflux conditions.

The aldehydic protons as a 1H singlet at δ 10.14, 10.00 ppm, additional presence of 2H singlet representing the benzylic protons present at δ 5.35, 5.30 ppm and appearance of aromatic protons at their respective positions of compounds **4a/4b** in the PMR spectrum. In the IR appearance of carbonyl stretching absorption strong bands at 1698, 1699 cm^{-1} and week bands at 3059, 3060 cm^{-1} due to fermi-resonance of C-H stretching of aldehyde, C-O-C stretching at 1245, 1247 cm^{-1} of compounds **4a/4b** along with the presence of $[M+1]^{\bullet+}$ peak at *m/z* 329, 362 in the mass spectrum respectively confirmed the structures assigned. The presence of 1H singlet at δ 9.90, 10.02 ppm for the aldehydic protons, additional presence of 2H singlet representing the benzylic protons present at δ 5.39, 5.45 ppm in the PMR spectrum, appearance of carbonyl stretching absorption strong bands at 1704, 1701 cm^{-1} and week doublet bands at 3065, 3061 cm^{-1} due to the fermi-resonance of C-H stretching

of aldehyde of compound **5a/5b** in FT-IR spectrum along with the presence of $[M+1]^{\bullet+}$ peak at *m/z* 313, 347 in the mass spectrum confirmed the structure assigned.

The synthesized aldehydes **4a/4b** and **5a/5b** was subjected to Knoevenagel condensation with methyl acetoacetate to obtain to obtain novel benzylidene based NCEs in **Schemes II** and **III**.

In the NMR spectra of methyl acetoacetate based targeted benzylidenes (**6a/6b** and **7a/7b**), the appearance of benzylidene protons 1H singlet signals in the region at δ 7.23, 7.88 ppm and at δ 7.58, 7.26 ppm, 3H singlet signals for the -O=C-O-CH_3 in the region at δ 3.58, 3.85 ppm and at δ 2.27, 3.86 ppm, 3H singlet signals for the methyl group in the region at δ 2.41, 2.38 ppm and at δ 1.95, 2.44 ppm confirmed, appearance of carbonyl stretching absorption strong bands at 1724, 1719 cm^{-1} and 1705, 1703 cm^{-1} **6a/6b** and **7a/7b**, respectively in NMR and IR spectrum confirmed the structure assigned. The presence of $[M+1]^+$ peak at *m/z* 427, 461 and at *m/z* 411, 445 in the mass spectrum of **6a/6b** and **7a/7b**, respectively provide additional support to the structure assigned to these molecules.

***In vitro* antioxidant activity:** The DPPH radical model is the most commonly used method for rapid evaluation of the free radical scavenging activity of organic compounds. The antioxidant activities of compounds **6a**, **6b**, **7a**, **7b** and ascorbic acid (standard) were assessed at different concentrations, with their EC_{50} values calculated to evaluate the potency of each compound (Table-1).

The antioxidant activities of compounds **6a**, **6b**, **7a**, **7b** and ascorbic acid (standard) were assessed at different concentrations, with their EC_{50} values calculated to evaluate the potency of each compound. As expected, ascorbic acid, a well-known antioxidant, showed significantly higher activity at all concentrations and the lowest EC_{50} value of 0.115 mM, indicating its superior antioxidant capacity compared to the other tested compounds. Among the synthesized compounds, **7b** demonstrated the highest antioxidant activity, particularly at higher concentrations, with an EC_{50} of 0.316 mM, slightly lower than the EC_{50} values of compounds **6a** (0.324 mM) and **7a** (0.327 mM). Compound **6b** also showed reasonable antioxidant potential, with an EC_{50} of 0.317 mM. These results suggest that both compounds **6b** and **7b** possess comparable antioxidant activity, slightly outperforming compounds **6a** and **7a**. However, compared to ascorbic acid, all four synthesized compounds exhibited lower antioxidant activities across the tested concentrations. This is clearly reflected in their higher EC_{50} values, which indicate that higher concentrations of these synthesized compounds are required to achieve the same level of antioxidant effect as ascorbic acid. The differences in activity among the compounds may be attributed to slight variations in their molecular structures, which could affect their ability to donate electrons or neutralize free radicals effectively.

DFT study

Structural optimization: The optimized structures of the synthesized compounds **6a**, **6b**, **7a** and **7b** are illustrated in Fig. 1. The geometry optimizations were performed using gradient corrected density functional theory (DFT) with the B3LYP method. All four compounds belong to the C1 point group. Compounds **6a** and **6b** each consist of 54 atoms, while **7a** and **7b** each consist of 53 atoms per molecule.

The calculated zero-point vibrational energies (ZPVE) for compounds **6a**, **6b**, **7a** and **7b** are 266.42, 260.40, 264.05 and 258.01 kcal/mol, respectively based on B3LYP/6-311G(d,p) optimizations. These values suggest that compounds with the oxygen linker (**6a**, **6b**) generally have higher ZPVE compared to those with a direct linker (**7a**, **7b**). This implies that the oxygen linker contributes to greater vibrational energy stabilization in the molecular structure. Similarly, the chlorobenzyl-substituted compounds (**6b**, **7b**) exhibit lower ZPVE than their benzyl counterparts, indicating that chlorine atom substitution reduced vibrational energy within the system.

The dipole moments of the synthesized compounds show slight variations: **6a** (4.0215 Debye), **6b** (4.1768 Debye), **7a** (3.6397 Debye) and **7b** (3.7457 Debye). This indicates that the compounds with the oxygen atom linker (**6a**, **6b**) exhibit higher dipole moments compared to those with a direct linker (**7a**, **7b**). Additionally, the presence of chlorobenzyl group (**6b**, **7b**) results in a greater dipole moment than compounds containing only a benzyl group (**6a**, **7a**).

Frontier molecular orbital (FMO) analysis: The HOMO-LUMO gap values and FMO structures for **6a**, **6b**, **7a** and **7b** molecules are shown in Fig. 2. It is observed that in all four molecules, the HOMO is predominantly localized on the hydrophobic region, specifically the benzimidazole ring. In contrast, the LUMO is distributed over the hydrophilic portion of the molecule, centered around the methylacetoacetate group. This distinct separation of electron density highlights the differential reactivity of these molecular regions. The synthesized benzimidazole derivatives (**6a**, **6b**, **7a** and **7b**) were evaluated for their electronic properties and antioxidant activities, providing insights into their reactivity and efficacy. The analysis of key parameters, including chemical potential (μ), electronegativity (χ), hardness (η), softness (S), electrophilicity index (ω) and HOMO-LUMO gap (Table-2), which reveals that compound **7b** exhibits the lowest chemical potential at -7.014 eV, indicating a greater tendency to stabilize with added electron density,

TABLE-1
EVALUATION OF *in vitro* ANTIOXIDANT ACTIVITY (DPPH ASSAY)

Compounds	Percentage (%) antioxidant activity at concentration (mM/L)					EC_{50} (mM)
	0.033 mM	0.067 mM	0.100 mM	0.133 mM	0.167 mM	
6b	2.01 ± 0.2	10.11 ± 0.3	14.11 ± 1.2	19.13 ± 0.5	25.01 ± 0.3	0.317 ± 0.005
7b	4.81 ± 0.8	12.13 ± 0.1	15.43 ± 0.2	21.92 ± 0.6	26.04 ± 0.1	0.316 ± 0.001
6a	3.91 ± 0.3	11.29 ± 0.3	13.11 ± 0.9	20.99 ± 0.7	25.15 ± 0.8	0.324 ± 0.005
7a	3.18 ± 0.5	12.01 ± 0.7	15.33 ± 1.0	21.33 ± 0.1	24.09 ± 0.7	0.327 ± 0.001
Ascorbic acid	14.39 ± 0.6	30.45 ± 0.7	41.66 ± 0.3	57.13 ± 0.6	73.11 ± 0.9	0.115 ± 0.000

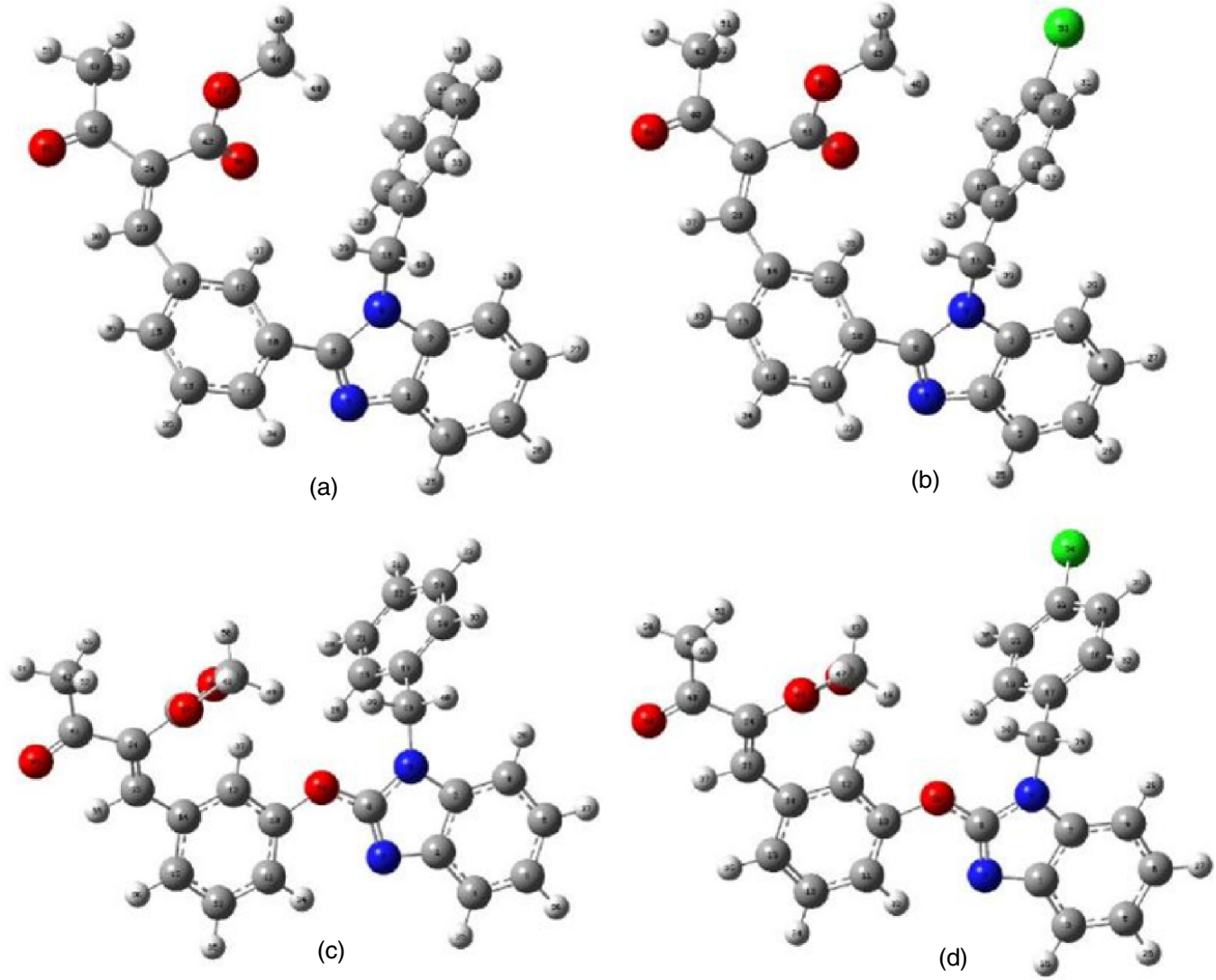

Fig. 1. Optimized geometric structure of (a) **7a**, (b) **7b**, (c) **6a**, (d) **6b** at b3lyp/6-311g(d,p) in the gas phase

TABLE-2
CHEMICAL REACTIVITY PARAMETERS

Molecule	HOMO-LUMO gap (eV)	Chemical potential (μ) (eV)	Electronegativity (χ) (eV)	Hardness (η) (eV)	Softness (S) (eV^{-1})	Electrophilicity index (ω) (eV)
7a	2.746	-7.303	7.303	1.373	0.728	19.42
7b	2.158	-7.014	7.014	1.079	0.927	22.80
6a	2.351	-7.034	7.034	1.175	0.851	21.05
6b	2.216	-7.259	7.259	1.108	0.903	23.77

suggesting enhanced antioxidant activity. This is further supported by its electronegativity value of 7.014 eV.

In terms of hardness and softness, compound **7a** has the highest hardness (1.373 eV), implying lower reactivity, whereas **7b** demonstrates a greater softness of 0.927 eV^{-1}, indicating a higher propensity to react with electrophiles. The balance between hardness and softness is critical, as softer molecules like **7b** tend to be more reactive, which correlates with its observed antioxidant activity in the DPPH assay.

The electrophilicity index (ω) provides additional context regarding the ability of these compounds to act as electrophiles, with values ranging from 19.42 eV to 23.77 eV. The higher electrophilicity of **7b** and **6b** suggests that while it may not be the most reactive as a nucleophile, it can still effectively engage with available electrons in free radicals, potentially enhancing its antioxidant properties. Furthermore, the HOMO-LUMO gap serves as a fundamental parameter reflecting the electronic transition energy and reactivity of the compounds. Compounds **7a** and **6a** show higher HOMO-LUMO gaps (2.746 eV and 2.351 eV, respectively), indicating lower reactivity in radical scavenging compared to **7b** and **6b**, which exhibit comparatively smaller gaps (2.158 eV and 2.216 eV, respectively). This observation correlates with the antioxidant activity results, where **7b** demonstrated superior scavenging efficiency. Overall,

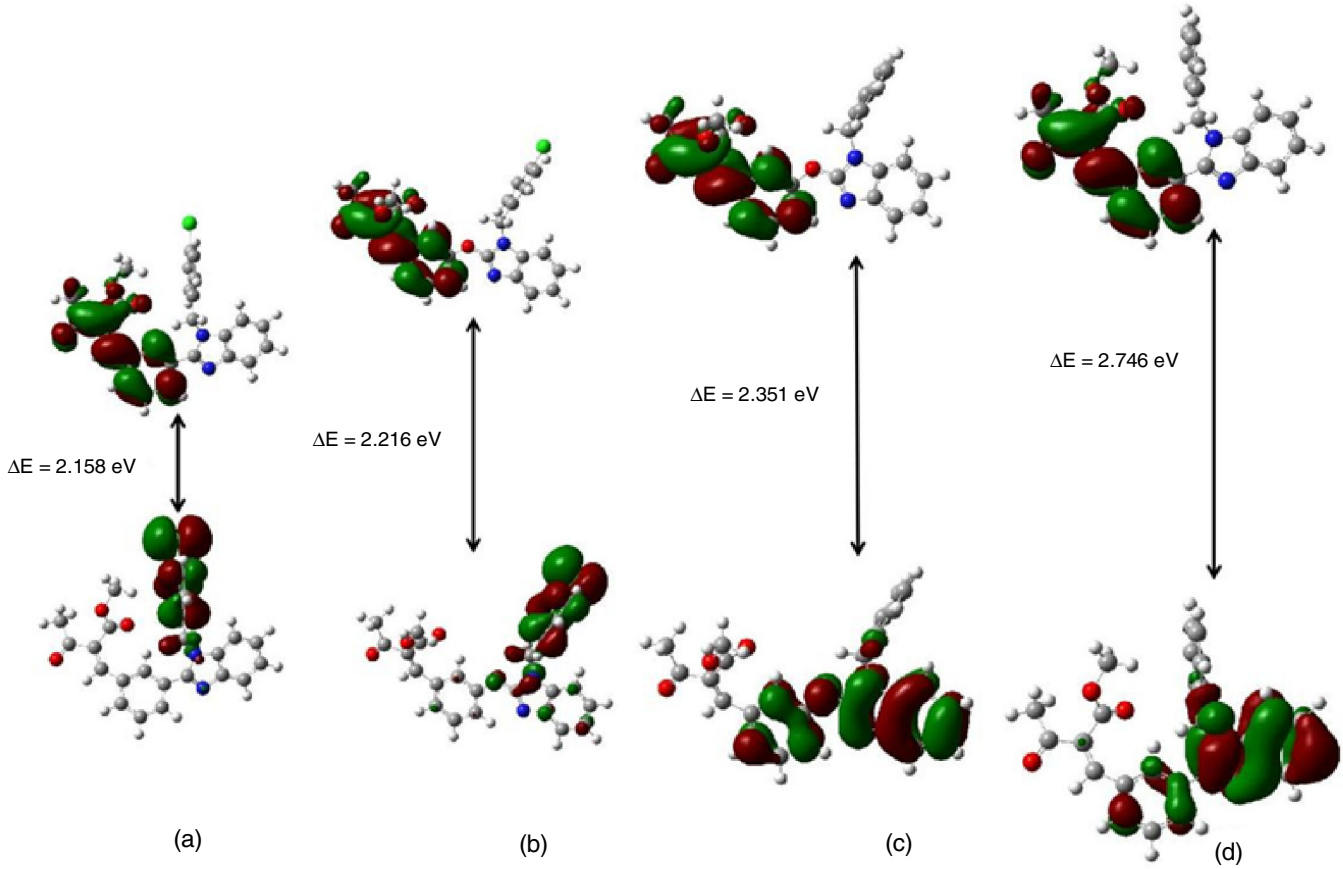

Fig. 2. HOMO and LUMO structure of (a) **7b**, (b) **6b**, (c) **6a**, (d) **7a** at b3lyp/6-311g(d,p) in the gas phase

the relationship between calculated electronic properties and experimental antioxidant activities highlights the potential of using DFT-derived parameters to predict reactivity. The DPPH assay results indicate that the compounds with smaller HOMO-LUMO gaps and higher softness show better radical scavenging capabilities, aligning with theoretical predictions. These findings underscore the utility of DFT calculations in predicting the reactivity and potential biological efficacy of novel compounds.

Comparison of experimental and theoretical NMR and FTIR: The correlation between experimental and computed chemical shifts for both ^{1}H NMR and FTIR is presented in Figs. 3 and 4, respectively. The squared correlation coefficient (R^2) values, obtained using the B3LYP method, are close to 1, indicating a strong agreement between the experimental and theoretical chemical shift values in case of NMR spectrum as well as the stretching/bending modes between different atoms in FTIR spectrum. This suggests that B3LYP provides reliable chemical shift predictions for the studied system.

Conclusion

This study successfully reports the synthesis and characterization of novel benzimidazole derivatives featuring methyl acetoacetate as a polar substituent, supported by a comprehensive analysis combining experimental and theoretical methodologies. The convergence of experimental findings, DFT studies and *in vitro* antioxidant assays revealed a strong correlation. All four compounds belong to the C1 point group, with ZPVE values of 266.42 (**6a**), 260.40 (**6b**), 264.05 (**7a**) and 258.01 kcal/mol (**7b**). Compounds with the oxygen linker (**6a**, **6b**) show both higher ZPVE (zero-point vibrational energy) and dipole moments than those with a direct linker, while chloro-benzyl substituted compounds (**6b**, **7b**) have higher dipole moments than their benzyl counterparts. The strong correlation ($R^2 \approx 1$) between experimental and computed chemical shifts in both ^{1}H NMR and FTIR spectra confirms that the B3LYP method provides accurate and reliable predictions for the studied system. The compound featuring direct linker chloro benzyl substituted benzimidazole based (**7b**), with the highest softness (0.927 eV^{-1}) along with dipole moment (3.7457 Debye) and the smallest HOMO-LUMO gap (2.158 eV), emerged as the most promising in terms of antioxidant potency (EC_{50} = 0.316 ± 0.001 mM), followed by **6b**, **6a** and **7a**. This research offers valuable insights into the effect of substitutions of the synthesized benzimidazole derivatives, highlighting their potential for future development of heterocyclic compounds.

ACKNOWLEDGEMENTS

The authors are thankful to the Punjabi University, Patiala authorities for providing the necessary research facilities. The athors are also grateful to Director and Mr. Avtar Singh of Sophisticated Analytical Instrumentation Facility (SAIF), Panjab University, Chandigarh, respectively, for extending the facilities for spectral analysis of the compounds reported in this artoc;es. Thanks are due to Dr. Harjinder Singh, Assistant Professor, Multani Mal Modi College, Patiala, for providing the Gaussian 09 facilities.

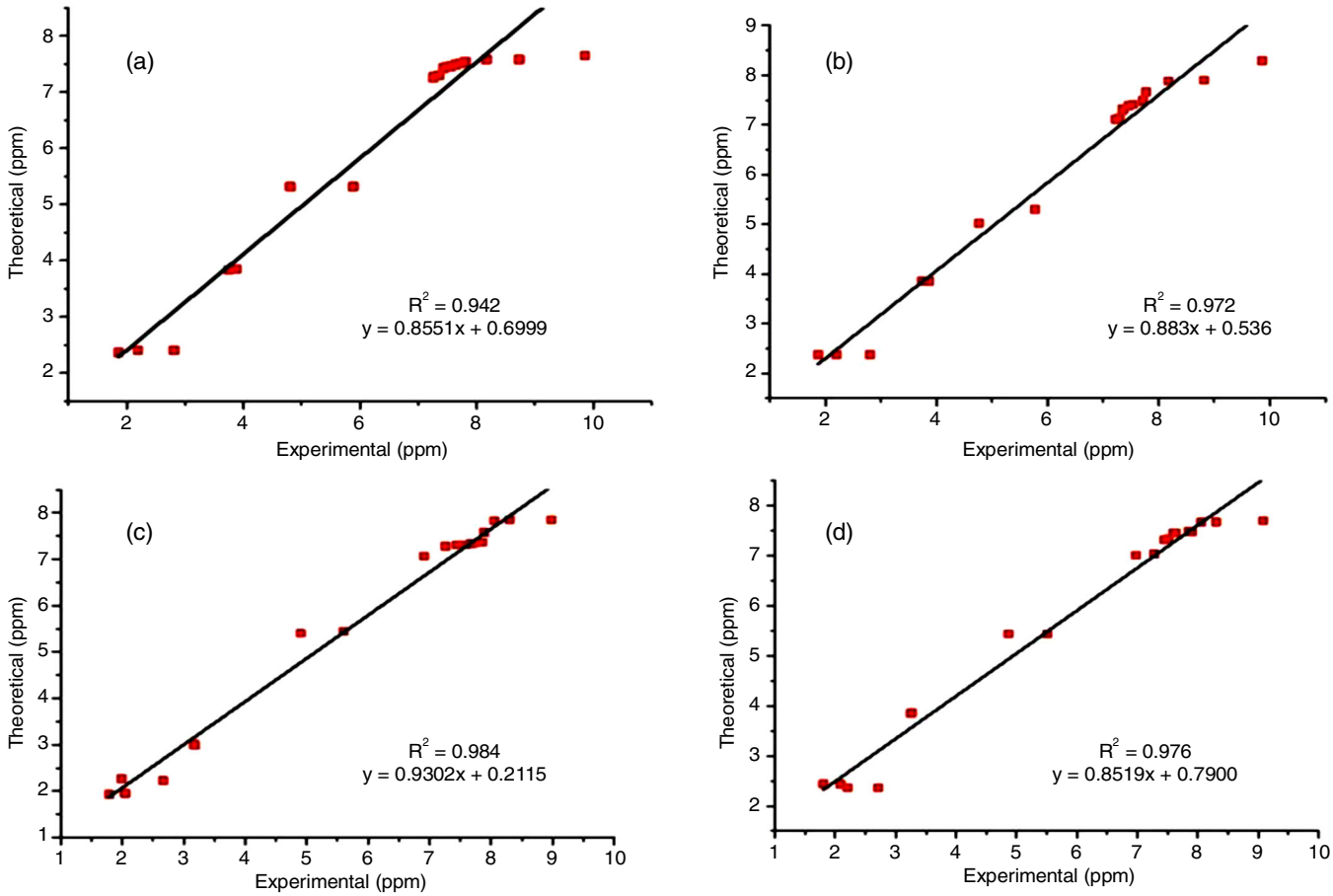

Fig. 3. Correlation graphs of experimental and theoretical ^{1}H NMR chemical shifts values (δ ppm) of (a) **6a**, (b) **6b**, (c) **7a**, (d) **7b** with GIAO-IEFPCM method in DMSO solvent

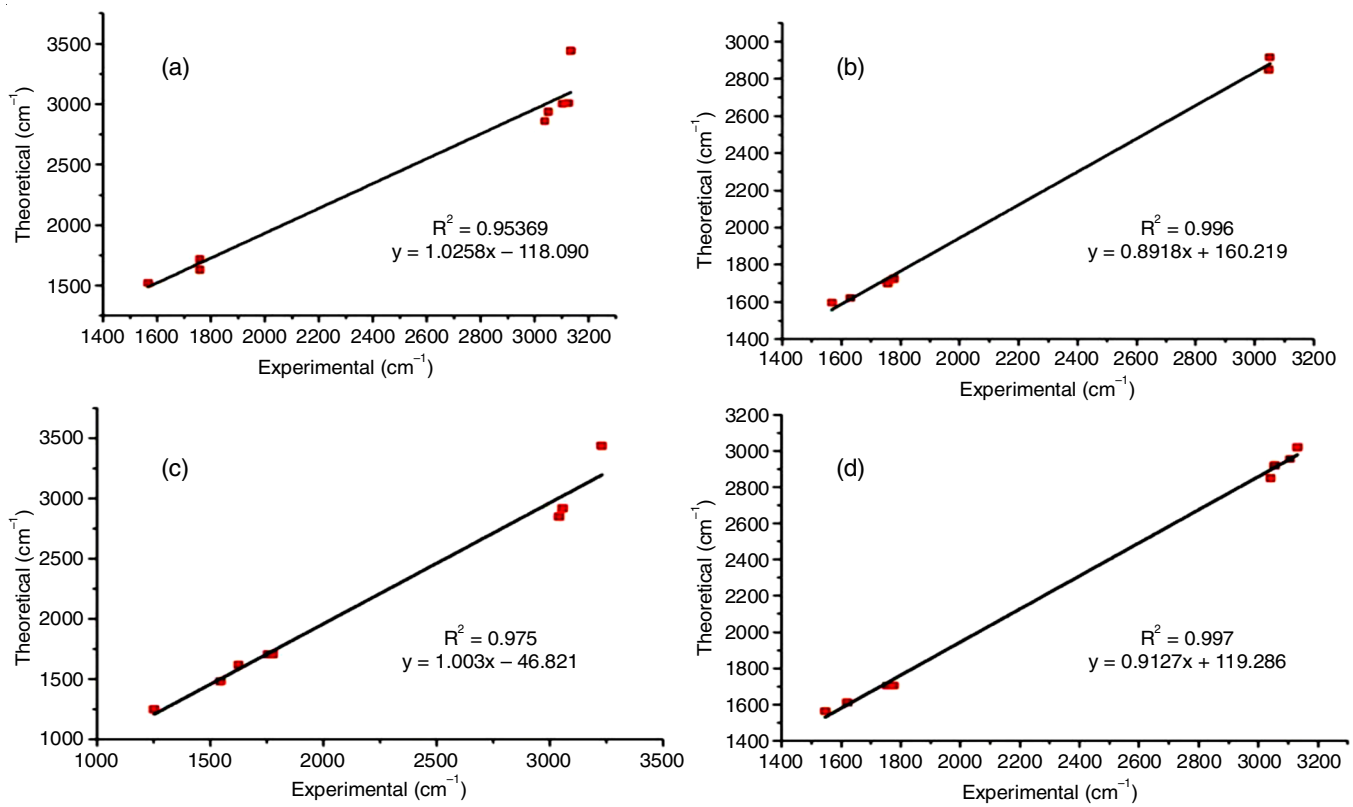

Fig. 4. Correlation graphs of experimental and theoretical FTIR frequency values of (a) **6a**, (b) **6b**, (c) **7a**, (d) **7b**

CONFLICT OF INTEREST

The authors declare that there is no conflict of interests regarding the publication of this article.

REFERENCES

1. S. Banerjee, S. Mukherjee, P. Nath, A. Mukherjee, S. Mukherjee, S.K. Ashok Kumar, S. De and S. Banerjee, *Results Chem.*, **6**, 101013 (2023); https://doi.org/10.1016/j.rechem.2023.101013
2. A. Choudhary, R.H. Viradiya, R.N. Ghoghari and K.H. Chikhalia, *ChemistrySelect*, **8**, e202204910 (2023); https://doi.org/10.1002/slct.202204910
3. H. Li, C. Gao, Z. Li, Y. Guo, S. Cao and Y. Zhao, *CrystEngComm*, 26, 5380 (2024); https://doi.org/10.1039/D4CE00714J
4. Y.H. Chen, C.H. Chen, C.M. Chang, B.A. Fan, D.G. Chen, J.H. Lee, T.L. Chiu, P.T. Chou and M.K. Leung, *J. Mater. Chem. C Mater. Opt. Electron. Devices*, **8**, 3571 (2020); https://doi.org/10.1039/C9TC06550D
5. E.O. Olufunmilayo, M.B. Gerke-Duncan and R.D. Holsinger, *Antioxidants*, **12**, 517 (2023); https://doi.org/10.3390/antiox12020517
6. A.V. Kozlov, S. Javadov and N. Sommer, *Antioxidants*, **13**, 602 (2024); https://doi.org/10.3390/antiox13050602
7. S.R. Brishty, M.J. Hossain, M.U. Khandaker, M.R.I. Faruque, H. Osman and S.M. Abdur Rahman, *Front. Pharmacol.*, **12**, 762807 (2021); https://doi.org/10.3389/fphar.2021.762807
8. H. Gurer-Orhan, H. Orhan, S. Suzen, M. Orhan Püsküllü and E. Buyukbingol, *J. Enzyme Inhib. Med. Chem.*, **21**, 241 (2006); https://doi.org/10.1080/14756360600586031
9. B.B. Kashid, A.A. Ghanwat, V.M. Khedkar, B.B. Dongare, M.H. Shaikh, P.P. Deshpande and Y.B. Wakchaure, *J. Heterocycl. Chem.*, **56**, 895 (2019); https://doi.org/10.1002/jhet.3467
10. M.A. Argirova, M.K. Georgieva, N.G. Hristova-Avakumova, D.I. Vuchev, G.V. Popova-Daskalova, K.K. Anichina and D.Y. Yancheva, *RSC Adv.*, **11**, 39848 (2021); https://doi.org/10.1039/D1RA07419A
11. G. Singh, A. Singh, V. Singh, R.K. Verma, J. Tomar and R. Mall, *Med. Chem. Res.*, **29**, 1846 (2020); https://doi.org/10.1007/s00044-020-02605-5
12. S. Aslam, M. Haroon, T. Akhtar, M. Arshad, M. Khalid, Z. Shafiq, M. Imran and A. Ullah, *ACS Omega*, **7**, 31036 (2022); https://doi.org/10.1021/acsomega.2c02805
13. K. Upendranath, T. Venkatesh, Y. Arthoba Nayaka, M. Shashank and G. Nagaraju, *Inorg. Chem. Commun.*, **139**, 109354 (2022); https://doi.org/10.1016/j.inoche.2022.109354
14. M.W. Wong, P.M. Gill, R.H. Nobes and L. Radom, *J. Phys. Chem.*, **92**, 4875 (1988); https://doi.org/10.1021/j100328a015
15. V. Singh, N. Sharma, A.K. Malik and S. Kaur, *J. Mol. Struct.*, **1294**, 136459 (2023); https://doi.org/10.1016/j.molstruc.2023.136459
16. S. Mahmoudi, M.M. Dehkordi and M.H. Asgarshamsi, *J. Mol. Model.*, **27**, 271 (2021); https://doi.org/10.1007/s00894-021-04891-1
17. R.K. Verma, R. Mall, P. Ghosh and V. Kumar, *Synth. Commun.*, **43**, 1882 (2013); https://doi.org/10.1080/00397911.2012.678461
18. G. Singh, A. Singh, R.K. Verma, R. Mall and U. Azeem, *Comput. Biol. Chem.*, **72**, 45 (2018); https://doi.org/10.1016/j.compbiolchem.2017.12.010